

## Dendritic polymer templates for the formation of nanoparticles in polymer matrix and their characterization

Ginam Kim\*\*, Franziska Gröhn\*, Brent Viers\*, Barry J. Bauer\*, C. L. Jackson\* and Eric J. Amis\*

\*\* Dow Corning Corp. C041D1

Midland, MI 48686

\*Polymers Division, National Institute of Standards and Technology, Gaithersburg, Maryland 20899

### Abstract

In this study, the morphological behavior of PAMAM dendrimers as stabilizers and templates for the formation of inorganic nanoclusters in amorphous and crystalline polymers is investigated using conventional transmission electron microscopy (TEM) and small angle X-ray scattering (SAXS). For the uniform dispersion in an amorphous interpenetrating polymer networks (IPN), the dendrimers were dissolved in 2-hydroxyethylmethacrylate (HEMA). In a second set of samples,  $\alpha$ - $\omega$  end-functionalized polyethylene glycol (PEG) was linked to the dendrimer terminal amino groups. For the synthesis of metal nanoclusters, the dendrimer-polymer networks swollen in water were placed into aqueous solutions of inorganic metal salts and the metal salts were washed out by water or hydrochloric acid. The network pieces were transferred into a solution of reducing agent, and then washed again with water, and dried in vacuum. TEM and SAXS data demonstrate the formation of nano-clusters in the uniformly dispersed PAMAM dendrimers in PHEMA IPN matrix. When PAMAM dendrimers are linked by crystallized PEG with spherulitic crystal structures, PAMAM dendrimers are incorporated in the inter PEG lamellar crystals with amorphous portion of PEG chains.

### Introduction

Dendrimers are recently developed highly branched polymers which are nearly monodisperse, highly functionalized and most often water soluble.(1,2) Various applications of dendrimers take advantage of the spherical shape, such as the use as covalently bonded micelles or as an agent for encapsulation ("dendritic box").(3) Some applications being investigated for dendrimers is related to the development of noble organic-inorganic hybrid materials having the combined properties of inorganic crystals with good mechanical and opto-electronic performances and organic compound with functionalities.(4,5) The unique ability of highly branched polyamidoamine (PAMAM) as stabilizers and templates for the formation of inorganic nanoclusters has been demonstrated.(6,7) In addition, because of biocompatibility and monodispersity, PAMAM dendrimers have been studied for biological applications; for example, the transfer of genetic materials in cells (8,9), or use of highly boronated, dendritic peptide makers for electron spectroscopy imaging of antigens. (10) To get desirable properties dendrimer blends with other polymer component, the morphological study of dendrimers in polymer matrix is necessary.

In this study, we investigate the quantum dot formation in PAMAM dendrimers and the morphological behavior of the dendrimers in amorphous interpenetrating polymer network (IPN) networks and crystalline polyethylene glycol (PEG) polymers using conventional transmission electron

microscopy (TEM) with staining and small angle X-ray scattering (SAXS).

### Experiment

PAMAM dendrimers were obtained from Dendritech (Michigan Molecular Institute, Michigan)(11) as a solution in methanol. To disperse dendrimers uniformly in an amorphous interpenetrating polymer networks (IPN), the monomer was dissolved in 2-hydroxyethylmethacrylate (HEMA) and the blends were polymerized. For the synthesis of metal nanoclusters, the dendrimer-polymer networks swollen in water were placed into aqueous solutions of inorganic metal salts for one week and the metal salts were washed out with water or hydrochloric acid. The network pieces were transferred into a solution of reducing agent, and then washed again with water, and dried in vacuum.

To observe the dendrimers in a crystallized polymer,  $\alpha$ - $\omega$  end-functionalized PEG ( $M_w=22000$  g/mol) was linked to the dendrimer terminal amino groups. Hydrolytically stable gels were formed by dissolving accurately weighted portions of PEG (95 %) and dendrimer (5 %) into polar solutions of water, methanol, or dimethyl sulfoxide. The quiescent mixtures were cured over the course of several hours in glass vials. To dry the samples, vacuum annealing was used.

SAXS data were collected at the Advanced Polymer Beam Line at Brookhaven National Laboratory, X27C as described elsewhere.(7) For TEM, cryo-microtomed electron transparent thin sections

were stained either by aqueous phosphotungstic acid (PTA) solution on Cu TEM grids or by exposing the sections to ruthenium vapor for 10 minutes and then the morphology was observed using a TEM. The measured diameters of various generations of dendrimers using SAXS and TEM are summarized in table 1

**Table 1. Size Measurements on PAMAM Dendrimers in IPN from TEM and SAXS (nm)**

Dendrimers	G8	G9	G10
The average size in IPN from TEM	9.6 ± 0.4	11.7 ± 0.8	14.7 ± 1.6
The average size in IPN from SAXS	9.6 ± 1.0		13.7 ± 1.4
The average size on a surface from TEM	10.2 ± 0.8	12.4 ± 0.5	14.7 ± 1.1
The average size in methanol from SAXS	10.4 ± 1.0	12.7 ± 1.3	14.8 ± 1.5

## Results and Discussion

The size, shape and distribution of PAMAM (G8, G9 and G10) dendrimers in IPN matrix are visualized by TEM after staining with the sodium salt of PTA (NaPTA), as shown in Figure 1. The differentially stained PAMAM dendrimers appear as dispersed particles with darker contrast than the IPN matrix without any significant agglomeration or clustering, as shown in Figure 1a-c for G8 to G10, respectively. The image contrast of dendrimers in TEM is due to the fact that NaPTA preferentially reacts with the amine groups in the PAMAM dendrimers rather than the IPN matrix. NaPTA is most widely used in negative staining biological systems, where an electron-dense heavy-metal salt in solution provides contrast by surrounding a small particle (12).

The area fraction of dispersed dendrimers to IPN matrix in the electron micrographs looks much higher than the real mass fraction of dendrimers in blends. This is because the microtomed thin sections (nominal thickness of 70 nm) are still much thicker than the dendrimer diameter, so that more than one layer of dendrimers can be projected into the resultant two-dimensional image. This may also result in overlapped dendrimers in some regions of the image. Even though some of dendrimers show a slight polyhedral shape, the typical shape of stained dendrimers in the IPN is roughly spherical.

The TEM results are well matched with previous SAXS data on these materials, but also demonstrate that large clumps or aggregates of dendrimers are not present. The average sizes of dendrimers in the IPN measured by TEM and the size data from SAXS are summarized in Table 1. The average sizes from TEM were obtained by measuring the diameters on a highly magnified electron micrograph and calculating the

mean value with  $\pm$  being one standard deviation. The average size measured by SAXS was obtained from a plot of the radius of gyration,  $R_g$ , of dendrimers in IPN and in solution with one standard deviation calculated as described elsewhere (13, 14).  $R_g$  was converted to a sphere radius assuming a uniform density sphere model,

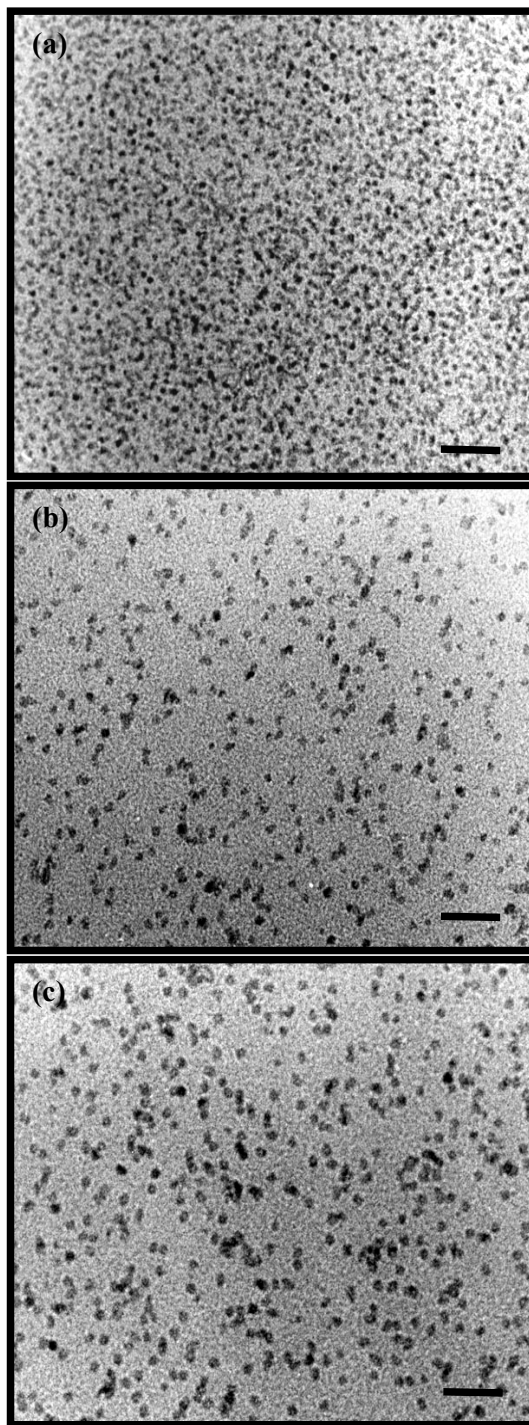


**Figure 1.** TEM images of PTA stained dendrimers in IPN; (a) 2 % G8 in IPN; (b) 1 % G9 in IPN; (c) 1 % G10 in IPN. The scale bars indicate 100nm.

as  $R = R_g/\sqrt{0.6}$ . The average sizes of the dendrimers in IPN measured using TEM are well matched with the values obtained from SAXS. This result is also consistent with the measured values for individual dendrimers in the absence of any solvent using TEM (15). As compared with the SAXS data, when the mass fraction of dendrimers is relatively low (1 % to 2 %), the average sizes of dendrimers in IPN and in methanol solution are nearly identical.

In crystallized PEG formed spherulitic crystal structures, PAMAM dendrimers are incorporated in the inter PEG lamellar crystals with amorphous portion of PEG chains (Figure 2). Figure 2a is the  $\text{RuO}_4$  stained image showing the center of a spherulite radiating crystal lamellae.  $\text{RuO}_4$  stained the amorphous regions having more free volume than chain folded crystal lamellae. In a crystallized PEG and G8 dendrimer blend, spherical dendrimers are distributed in amorphous regions between PEG lamellar crystals, as shown in a PTA stained image of Fig. 2b.

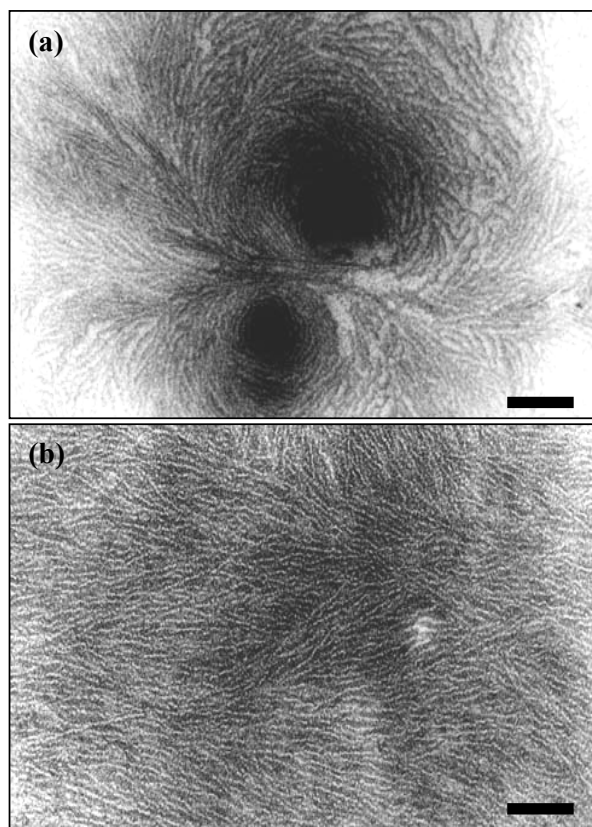


**Figure 2.** TEM images of G8 dendrimers in PEG formed spherulites; (a)  $\text{RuO}_4$  stained; (b) PTA stained; the scale bars indicate 250 nm

Figure 3 shows SAXS results for dendrimer-polymer networks containing a mass fraction of 1% dendrimers generation 7 to 10 (G7 to G10) after loading with  $\text{H}_2\text{PtCl}_6$ . The uncertainties of the data presented

are estimated as the standard deviation of the mean and are smaller than the plotted points and are not shown for clarity. The scattering curves exhibit the features typical of the form factors of these higher generation dendrimers in solution, i.e., sphere form factors.(13) This result demonstrates that the  $\text{PtCl}_6^{2-}$  ions are indeed accumulated inside the dendrimer. In addition, it can be seen from the scattering curves that the dendrimers are well-dispersed inside the polymer matrix and no aggregates are detected. This is in agreement with SAXS and TEM characterization of these unmodified dendrimer-polymer networks under staining with phosphotungstic acid. (16) The same result is found for loading the networks with copper ions.

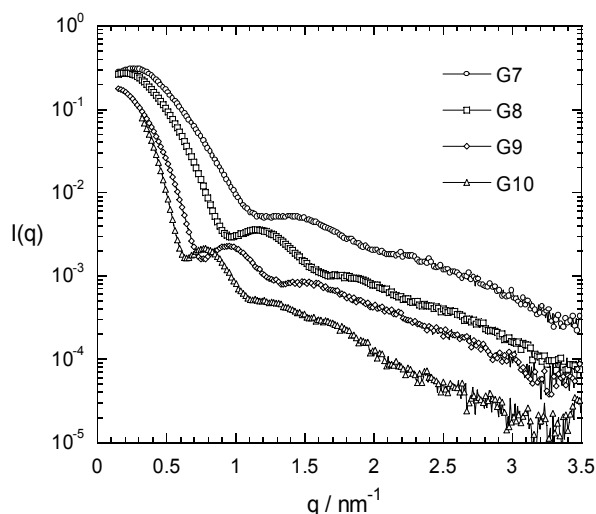


**Figure 3.** SAXS of dendrimer-polymer networks containing a mass fraction of 1% dendrimers generation 7 to 10 after loading with  $\text{H}_2\text{PtCl}_6$

When swollen in aqueous solution, metal ions were attached to the dendrimers dispersed in IPN matrix. Chemically reducing these metal ions results in nano-metal clusters that are located inside the dendrimers, as shown in Figure 4. Reduction of metal salt inside the polymer-dendrimer network results in metal clusters of nanometer size, as can be seen by the dark red or brown color of the polymer network for the gold and the platinum samples, respectively. For G7 and G8, the size of the metal nanoclusters is controlled by the maximum number of metal ions that can be electrostatically attached. For G9 and G10, multiple colloidal particles per dendrimer are formed, due to the crowded conditions inside the dendrimer and the influence of the polymer matrix. TEM images of Pt colloids obtained upon reduction of a polymer-dendrimer network show that the metal colloids that are formed are well-dispersed in the polymer matrix, as shown in Figure 4. The formation of Pt nanoclusters in a polymer composite of mass fraction 1 % G9 PAMAM dendrimers and PHEMA is confirmed by unstained TEM image revealing the dark contrast of Pt

nanoparticles in the matrix (Fig. 4a). PTA stained image clearly demonstrated that Pt colloids revealing dark contrast are formed inside of G9 PAMAM dendrimers having gray contrast in PHEMA matrix, as shown in Figure 4b.

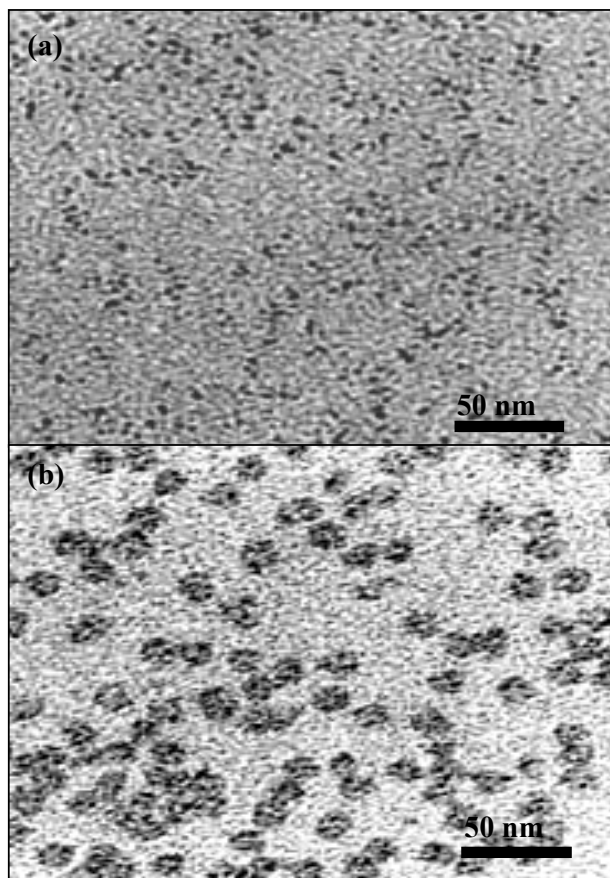


**Figure 4.** TEM images of (a) PTA stained G9 dendrimers in poly(hydroxyethyl methacrylate) (PHEMA); (b) Pt nanocolloids formed in a G9 dendrimers/PHEMA composite; (c) after PTA staining the sample imaged in (b)

### Summary

PAMAM dendrimers are visible as individual molecules as observed by TEM of thin sections stained with NaPTA. The TEM results are consistent with previous SAXS data on these materials without demonstrating the presentation of large clumps or aggregates of dendrimers. As compared with the average size of dendrimers in solution, using the polymeric matrix as a host for the dendrimers does not appear to affect the size and shape of dendrimers at relatively low-mass fraction of dendrimers.

When the polymer matrix is crystallized and form spherulitic structure, PAMAM dendrimers are distributed in the inter PEG lamellar amorphous regions with PEG amorphous proton.

Nano-metal clusters from chemical reduction of metal ions in the dendrimer-IPN composites are located inside the dendrimers. For G9 and G10, multiple colloidal particles per dendrimer are formed, as can be understood by the volume conditions inside the dendrimer and the additional influence of the polymer matrix.

### References:

1. Tomalia, D. A.; Baker, H.; Dewald, J.; Hall, M.; Kallos, G.; Martin, S.; Roeck, J.; Ryder, J.; Smith, P. *Macromolecules* **1986**, *19*, 2466-2468.
2. Tomalia, D. A.; Naylor, A. M.; Goddard, W. A. *Angewandte Chemie-International Edition in English* **1990**, *29*, 138-175.
3. Jansen, J.; Meijer, E. W.; deBrabandervandenBerg, E. M. M. *Macromolecular Symposia* **1996**, *102*, 27-33.
4. Aiken, J. D.; Finke, R. G. *Journal of Molecular Catalysis a-Chemical* **1999**, *145*, 1-44.
5. Mazzoldi, P.; Arnold, G. W.; Battaglin, G.; Gonella, F.; Haglund, R. F. *Journal of Nonlinear Optical Physics & Materials* **1996**, *5*, 285-330.
6. Gröhn, F.; Bauer, B. J.; Akpalu, Y. A.; Jackson, C. L.; Amis, E. J. *Macromolecules* **2000**, *33*, 6042-6050.
7. Gröhn, F.; Kim, G.; Bauer, B. J.; Amis, E. J. *Macromolecules*, **2001**, *34*, 2179
8. Kuskowskalatallo, J. F.; Bielinska, A. U.; Johnson, J.; Spindler, R.; Tomalia, D. A.; Baker, J. R. *Proc. Natl. Acad. Sci. USA*, **1996**, *93*, 4897.
9. Plank, C.; Mechtler, K.; Szoka, F. C.; Waqner, E. *Hum. Gene Ther.* **1996**, *7*, 1437.
10. Qualman, B.; Kessels, M. M.; Klobasa, F.; Jungblut, P. W.; Sierrata, W. D. *J. Microsc.* **1996**, *183*, 69.
11. Note: *Certain commercial materials and equipment are identified in this paper in order to specify adequately the experimental procedure. In no case does such identification imply recommendation by the National Institute of Standards and Technology nor does it imply that the material or equipment identified is necessarily the best available for this purpose.*
12. Harris, J. R. *Negative Staining and Cryoelectron Microscopy: The Thin Film Techniques*; Bios Scientific Publishers: Oxford, U. K., 1997.
13. Prosa, T. J.; Bauer, B. J.; Amis, E. J.; Tomalia, D. A.; Scherrenberg, R. *Journal of Polymer Science Part B-Polymer Physics* **1997**, *35*, 2913-2924.
14. Bauer, B. J.; Prosa, T. J.; Liu, D.; Jackson, C. L.; Tomalia, D. A.; Amis, E. J. *American*

*Chemical Society, Polymer Preprints* **1999**, *40*, 406.

15. Jackson, C. L.; Chanzy, H. D.; Booy, F. P.; Drake, B. J.; Tomalia D. A.; Bauer, B. J.; Amis, E. J. *Macromolecules* **1998**, *31*, 6259.
16. Bauer, B.J.; Prosa, T.J.; Kim, G.; Jackson, C.L.; Liu, D.W.; Amis, E.J.; in preparation.